# Structural, electrical transport and x-ray absorption spectroscopy studies of $LaFe_{1-x}Ni_xO_3$ ($x \leqslant 0.6$)

Ravi Kumar[a] and R. J. Choudhary
*Nuclear Science Center, Aruna Asaf Ali Marg, New Delhi 110067, India*

M. Wasi Khan and J. P. Srivastava
*Department of Physics, Aligarh Muslim University, Aligarh 202002, India*

C. W. Bao, H. M. Tsai, J. W. Chiou, K. Asokan,[b] and W. F. Pong
*Department of Physics, Tamkang University, Tamsui 251, Taiwan*

(Received 21 May 2004; accepted 10 February 2005; published online 22 April 2005)

Electronic structures of $LaFe_{1-x}Ni_xO_3$ ($x \leqslant 0.6$) have been studied by x-ray absorption near edge structure spectra of O *K*, Fe $L_{2,3}$ and La $M_{4,5}$ edges. Upon substitution of Ni at Fe site in $LaFeO_3$, the O *K*-edge spectra show a feature about 2.0 eV lower than that of $LaFeO_3$. This feature is growing as the concentration of Ni is increasing. This is consistent with our resistivity data which show that the resistivity decreases very fast with Ni substitution from GΩ cm for $LaFeO_3$ to a few mΩ cm for the sample with 60% Ni substitution. The resistivity data have been fitted with a variable-range hopping model and it is found that the gap parameter reduces from 2 eV to 2.1 meV with the Ni substitution. This gap parameter decreases very systematically with the increase in Ni concentration. The structural analysis of these samples shows that they have single-phase orthorhombic structure with space-group *Pnma* in the studied range ($0 \leqslant x \leqslant 0.6$). The study of Fe $L_{2,3}$-edge structures confirm the trivalent state of Fe. The observed features have been explained on the basis of charge-carrier doping in $LaFeO_3$. The disorder-induced localization is found to effectively control the resistivity behavior. © *2005 American Institute of Physics*. [DOI: 10.1063/1.1884754]

## I. INTRODUCTION

During the last few decades, there has been a resurgence of interest in the study of the transition-metal oxides (TMO) which exhibit a spectacular variety of inspiring physical properties, such as dielectric, magnetic, optical, and transport properties, owing to the strong electron-correlation effect in the system. The discovery of high-$T_c$ superconductivity[1] in cuprate systems, metal-insulator (MI) transition, colossal magneto resistance, and charge ordering in manganites[2] and many other phenomena in other TMO systems further regenerated the efforts to understand the electronic structure of TMO and the effect of disorder on the electronic correlation effects. Most of these properties are due to the close interplay between the magnetic and electronic properties arising from the simultaneous presence of strong electron-electron interaction potential within the transition metal *d* orbital and a sizeable hopping interaction between the transition metal *d* and oxygen *p* orbitals. During the past few years, many efforts have been attributed to understand the electronic structure of perovskite-based TMO systems, such as $LaFeO_3$, $LaCoO_3$, $LaCrO_3$, $LaNiO_3$, and $LaMnO_3$,[3–6] and also of doped manganites.[7–11] It is appealing to note that while $LaNiO_3$ has rhombohedral perovskite structure and is a Pauli-paramagnetic metal with high electrical conductivity at room temperature,[12] the other TMO systems are generally insulators. This provides an interesting occurrence of MI transition as one goes from $LaNiO_3$ to the end member of another TMO system (for instance $LaFeO_3$) at a critical substitution concentration of the corresponding transition-metal element (viz., Fe in $LaNi_{1-x}Fe_xO_3$).[13,14] This presents a prospect to explore Mott's criteria of dependence of MI transition on the critical charge-carrier density by moving in one such series from one end member of $LaNiO_3$ to the other. It has also been recognized that the MI transition phenomena, occurring in the mixed systems, correspond to the structural transition as well.[3] These aspects have generated several motivating studies in this direction in the mixed composition of $LaNi_{1-x}M_xO_3$ ($M$=Cr, Mn, Fe, or Co).[15–17] In the present study we report our observations of the dependence of Ni concentration on the electrical and structural evolution in the $LaFe_{1-x}Ni_xO_3$ ($0 \leqslant x \leqslant 0.6$) compound in the semiconducting substitutional range. The semiconducting region in the composition has been chosen with the incentive to avoid any disorder effects due to the structural transition.

$LaNiO_3$ has the carrier density of about $8 \times 10^{18}$ $cm^3$ and is electrically conducting at room temperature.[1,2] On the other hand, $LaFeO_3$, having orthorhombic perovskite structure, is an insulator and shows weak ferromagnetic transition at Néel temperature $T_N \sim 750$ K.[18] Rao *et al.*[15] have shown that in the $LaNi_{1-x}Fe_xO_3$ series, with the increase in Fe concentration, the itinerancy of *d* electrons decreases and these oxides become semiconducting for Fe concentration higher than 20%. They also observed that structural transition takes place from rhombohedral ($LaNiO_3$) to orthorhombic

[a]Author to whom correspondence should be addressed; electronic mail: ranade@nsc.ernet.in
[b]Permanent address: Nuclear Science Center, New Delhi 110067, India.

 

($LaFeO_3$) at Fe concentration of ~50% or above in $LaNiO_3$. Ganguly *et al.*[13] studied the series of $LaNi_{1-x}M_xO_3$ ($M$=Cr, Mn, Fe, or Co), observing that there was a characteristic critical composition ($x_c$) to bring in transition from metallic to nonmetallic status. For Fe-substituted series, they too reported the structural transition as Rao *et al.*[15] did, and the $x_c$ was in the range of $0.25 < x_c < 0.35$. The reported $x_c$ was different for different transition-metal elements, indicating the MI transition to be due to disorder effects. Chainani *et al.*[14] reported in their work that the semiconducting compositions ($Fe \geqslant 0.3$) exhibit variable-range hopping (VRH) model at high temperatures, confirming the role of disorder in causing the MI transition. The electronic structures of the $LaNi_{1-x}M_xO_3$ ($M$=Mn, Fe, and Co) series have been investigated by Sarma *et al.*[16] with the help of x-ray absorption spectroscopy (XAS) at the oxygen *K*-edge. They suggested that in these systems the MI transition is due to the potential mismatch between the substituent metal ion and $Ni^{+3}$ ion which causes the transferring of hole states from near $E_F$ to an energy position above $E_F$. Recently, Massa *et al.*[19] have studied in detail the infrared properties of $LaNi_{1-x}Fe_xO_3$ to understand the phonon structure yields to the carrier contributions as the system undergoes metal-to-insulator behavior. With these reports available in the literature, it seems that the series has been well studied across the metallic phase of $LaNiO_3$ to the insulating phase of $LaFeO_3$. However, it would be useful to study systematically the dependence of Ni concentration on the evolution of electronic phase vis-à-vis the effect of disorder on the electronic property of the $LaFe_{1-x}Ni_xO_3$ series while remaining in the semiconducting region of the composition (i.e., without crossing the critical composition for the insulator-to-metal transition). In the present paper, we have investigated the electrical transport and the crystallographic and electronic structure of $LaFe_{1-x}Ni_xO_3$ ($x \leqslant 0.6$). The emphasis is on the understanding of its electronic properties and electronic structure in a stable phase.

## II. EXPERIMENT

The samples of $LaFe_{1-x}Ni_xO_3$ ($0 \leqslant x \leqslant 0.6$) were synthesized using standard solid-state reaction technique. The stoichiometric amounts of high-purity $La_2O_3$, FeO, and NiO powders were mixed thoroughly and precalcinated for 12 h at 1000 °C. The precalcinated materials were again ground and calcinated at 1250 °C for 24 h. Finally, the samples were ground to fine powder, pressed to the pellet form, and sintered at 1300 °C for 24 h. This sintering procedure was repeated three times to get the better homogeneity in the samples. Powder x-ray diffraction measurements were performed using Philips diffractometer PW 3020 with Cu $K\alpha$ radiation at room temperature. All the samples exhibit single-phase orthorhombic structure. Electrical resistivity measurements were performed using standard four-probe technique in the temperature range 9–300 K using a close-cycle refrigerator (CTI 8200), and the temperature was controlled at ±50 mK using a Lakeshore temperature controller. All the resistivity measurements were carried out in the warm-up cycle. The x-ray absorption measurements on these samples along with $Fe_2O_3$ and NiO at O *K*, Fe $L_{2,3}$, and La $M_{4,5}$ edges were made using the high-energy spherical grating monochromator (HSGM) beam line of the National Synchrotron Radiation Research Center (NSRRC), Taiwan, operating at 1.5 GeV with a maximum storage current of 200 mA. The spectra were measured using the sample drain current mode at room temperature and the vacuum in the experimental chamber was in low range of $10^{-9}$ torr. The resolution of the spectra was better than 0.2 eV.

## III. RESULTS AND DISCUSSION

### A. X-ray diffraction (XRD)

Figures 1(a) and 1(b) show the experimental and calculated XRD patterns using Rietveld refinement technique for $LaFe_{1-x}Ni_xO_3$ ($x$=0, 0.1, 0.3, 0.4, 0.5, and 0.6) samples. The analysis of powder XRD patterns at room temperature shows that all the samples are formed in single phase with orthorhombic crystal symmetry having space group *Pnma*. However, as the concentration of Ni substitution increases to 0.5 and above, the line widths as well as the difference between the intensities of the measured and calculated spectra increase. It indicates that the system is getting distorted and the crystal symmetry is approaching its form to the point of a phase transformation. Hence, we can say that the samples exhibit single-phase orthorhombic crystal symmetry below 60% Ni substitution, which is in agreement with the results[12,15,19–21] reported earlier. Table I gives the calculated lattice parameters and the unit-cell volume for these samples. It is clearly evident from these values that parameter *a* is decreasing with the increase in Ni concentration, whereas parameter *b* shows only a slight decrease for the sample with 50% Ni substitution and parameter *c* shows a small irregular variation. The overall unit-cell volume is found to decrease with the increase in Ni concentration, obviously because of the replacement of $Fe^{+3}$ (high spin) with $Ni^{+3}$ (low spin) having a smaller radius. From these observations we find that, in this substitution range, our samples are in single phase with orthorhombic structure.

### B. Electrical resistivity

In order to understand the effect of the carrier doping by Ni substitution in $LaFeO_3$, we have measured the electrical resistivity as a function of temperature in the temperature range 9–300 K. The pure $LaFeO_3$ sample shows resistivity around GΩ cm at room temperature, and at low temperature it is immeasurably high, showing that the sample is insulator. Figure 2 shows the resistivity as a function of temperature for the samples $LaFe_{1-x}Ni_xO_3$ ($x$=0.1, 0.2, 0.3, 0.4, 0.5 and 0.6). It is clearly evident in the plots that the resistivity at room temperature is decreasing with increasing Ni substitution, and for 60% Ni substitution it drops to 5 mΩ cm at room temperature, which is a demonstration of their semiconducting nature. It is evident that the resistivity value spans in the range of a few GΩ cm to 5 mΩ cm (a change of 12 orders of magnitude) as one goes from $LaFeO_3$ to $LaFe_{0.4}Ni_{0.6}O_3$. To understand this nature of resistivity data, we have analyzed our results in Mott's variable-range hopping (VRH) model. Figure 3 shows the ln $\rho$ versus $T^{-1/4}$ plot

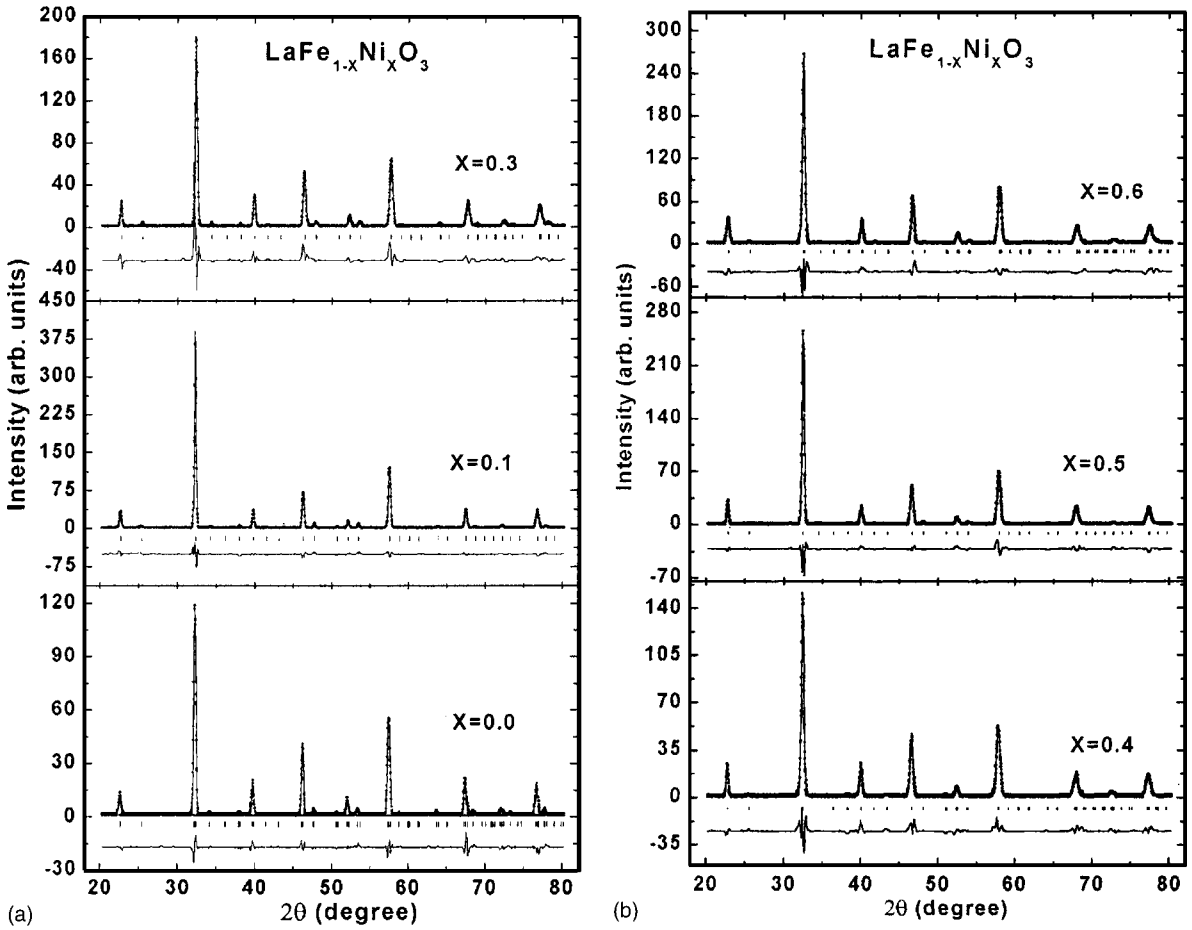


FIG. 1. (a) XRD pattern of the compound $LaFe_{1-x}Ni_xO_3$ ($x=0.0$, 0.1, and 0.3). Dots plus line indicate the experimental data, and calculated profile is the line overlying them. The lowest curve shows the difference between experimental and calculated patterns. The vertical bars indicate the expected reflection positions. (b) XRD pattern of the compound $LaFe_{1-x}Ni_xO_3$ ($x=0.4$, 0.5, and 0.6). Dots plus line indicate the experimental data, and calculated profile is the line overlying them. The lowest curve shows the difference between experimental and calculated patterns. The vertical bars indicate the expected reflection positions.

for all the samples. These plots reveal that higher temperature data fit very well with VRH model. The slope of the curve decreases with the increase in the Ni concentration, which indicates that the activation energy or overall hopping potential decreases with the carrier doping via Ni substitution. Table II shows the temperature down to which the VRH model fits the data well, the resistivity value at the lower limit of temperature, and the activation energy calculated using the VRH model. It has been noticed that the activation energy decreases very fast with the Ni substitution from 9.10 meV (for 10% Ni) to 2.15 meV (for 60% Ni), whereas for pure $LaFeO_3$ it is around 2 eV (reported in literature[6] and also shown by our XAS data; see next section). These observations are consistent with the earlier reported data in the literature wherein it has been suggested that, as long as the members of this series are in semiconducting region, they obey the VRH model over a limited range of temperature.[15,13] This observation indicates that the electronic property in the system is driven by the induced disorder effect due to the presence of two different homovalent transition-metal elements (Fe and Ni). It can be explained on the basis that pure $LaNiO_3$ has a carrier density around $8\times10^{18}$ $cm^3$. As we are substituting the Ni in $LaFeO_3$, we are doping the carrier in the system; for example, we have doped the carrier in the range $8\times10^{17}$ (for 10% Ni) to $4.8\times10^{18}/cm^3$ (for 60% Ni). This increase in carrier density in

TABLE I. The lattice parameters and the unit-cell volume for different compositions of $LaFe_{1-x}Ni_xO_3$ ($x=0.0$, 0.1, 0.3, 0.4, 0.5, and 0.6).

| Composition | Crystal symmetry | a (Å) | b (Å) | c (Å) | Unit cell volume ($Å^3$) |
|---|---|---|---|---|---|
| $LaFeO_3$ | Orthorhombic | 5.57111 | 7.87368 | 5.53483 | 242.786 |
| $LaFe_{0.9}Ni_{0.1}O_3$ | Orthorhombic | 5.55485 | 7.85359 | 5.55254 | 242.233 |
| $LaFe_{0.7}Ni_{0.3}O_3$ | Orthorhombic | 5.53904 | 7.81601 | 5.53835 | 239.773 |
| $LaFe_{0.6}Ni_{0.4}O_3$ | Orthorhombic | 5.53221 | 7.80138 | 5.51003 | 237.804 |
| $LaFe_{0.5}Ni_{0.5}O_3$ | Orthorhombic | 5.51897 | 7.80099 | 5.50539 | 237.025 |
| $LaFe_{0.4}Ni_{0.6}O_3$ | Orthorhombic | 5.49442 | 7.80367 | 5.52043 | 236.698 |

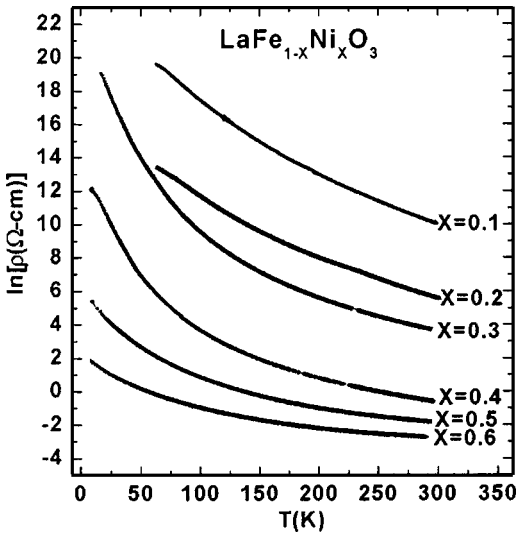


FIG. 2. Resistivity as a function of temperature for different compositions of $LaFe_{1-x}Ni_xO_3$ ($x=0.1$ to 0.6).

the system decreases its energy gap. ln general, for these systems the degeneracy level reaches around $N_c=5\times10^{18}$ cm$^3$ and so we can say that with 63% Ni substitution the system will undergo insulator-to-metal transition (also observed from earlier reported electrical resistivity measurement[13,14] and infrared reflectivity studies by Massa *et al.*[19]) The decrease in the gap parameter can also indicate that the correlation length in the conducting network is increasing. These result, together with the VRH model, tend to suggest that the conduction in these materials is governed by the disorder-induced localization of charge carriers, as also proposed by Sarma *et al.*[17] in $LaNi_{1-x}M_xO_3$ ($M$=Mn and Fe) and MacEachern *et al.*[22] in $LaTiO_3$.

### C. X-ray absorption spectroscopy

We have measured the x-ray absorption spectra at O $K$ edge and Fe $L_{2,3}$ edges. To investigate the electronic structure of $LaFe_{1-x}Ni_xO_3$ close to Fermi level, which is dominated by the transition metal 3$d$ and O 2$p$ states. Figure 4 shows the normalized spectra measured at O $K$ edge for $LaFe_{1-x}Ni_xO_3$ samples for $x=0$ to $x=0.5$ at room temperature (300 K). The spectra of NiO and $Fe_2O_3$ are also shown in Fig. 4 for comparison. These spectra are normalized to have the same area in the energy range of 550–560 eV (not fully shown) after following the standard procedure for background subtraction. It is well known that the x-ray absorption spectra at O $K$ edge probe the unoccupied states with the O 2$p$ symmetry due to the dipole selection rules. This arises mainly from the hybridization of O 2$d$ states with the different states of neighboring atoms, namely, the 3$d$ state of Fe and Ni and also the $d$ state of La in the present case. First of all, we would like to understand the spectrum of pure $LaFeO_3$. The well-defined doublet in the spectrum of pure $LaFeO_3$ marked $a$ and $a'$ arises from the covalent or hybridization mixing of $p$ states of oxygen with the Fe $d$ density of states. They may occur due to the crystal-field splitting of Fe 3$d$ level in $t_{2_g}$ and $e_g$ levels by the presence of local cubic field around the Fe site. In the energy region of 534–537 eV

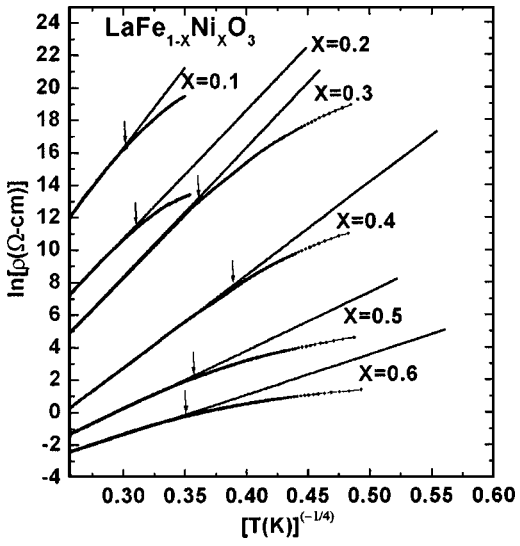


FIG. 3. Plot of $\ln\rho$ against $T^{-1/4}$ of the resistivity data for samples $LaFe_{1-x}Ni_xO_3$ ($x=0.1$ to 0.6). Line plus dot indicate the experimental data, while solid line shows the calculated linear fit in the variable-range hopping model.

TABLE II. Resistivity and activation energy for different compositions of $LaFe_{1-x}Ni_xO_3$ ($x=0.1$ to 0.6).

| Composition | [a]$T_d$ | $\rho(\Omega$ cm) at $T_d$ | $E_c$ (meV) |
|---|---|---|---|
| $LaFe_{0.9}Ni_{0.1}O_3$ | 142.41 | $4.5739\times10^{6}$ | 9.10 |
| $LaFe_{0.8}Ni_{0.2}O_3$ | 114.54 | $6.8347\times10^{4}$ | 6.84 |
| $LaFe_{0.7}Ni_{0.3}O_3$ | 54.76 | $6.6812\times10^{4}$ | 6.63 |
| $LaFe_{0.6}Ni_{0.4}O_3$ | 55.97 | $6.2090\times10^{2}$ | 4.90 |
| $LaFe_{0.5}Ni_{0.5}O_3$ | 75.29 | $5.2021\times10^{0}$ | 3.09 |
| $LaFe_{0.4}Ni_{0.6}O_3$ | 85.22 | $5.3001\times10^{-1}$ | 2.14 |

[a]The temperature below which VRH model is not applicable.

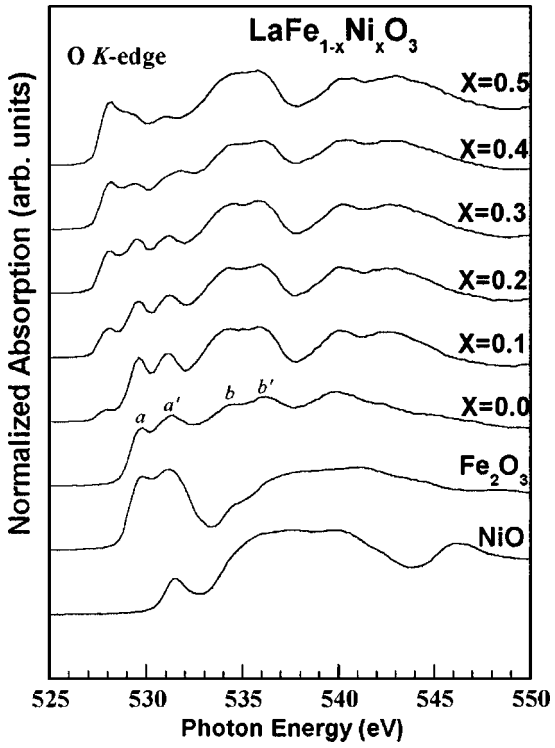


FIG. 4. Normalized O $K$-edge XAS spectra of $LaFe_{1-x}Ni_xO_3$ ($x=0.0$ to 0.5).

the features marked as $b$ and $b'$ can be assigned to the mixed states of O $2p$ and La $d$ state, whereas the broad features in higher-energy region may be attributed to the mixing of Fe $4sp$ and La $5sp$ states. All these features observed in the pure $LaFeO_3$ spectrum are consistent with the reports of earlier workers.[7,23]

Now, we discuss the spectra of Ni-substituted $LaFeO_3$ samples. It has been noticed that in the spectrum for $x=0.1$ (10% Ni substitute) a small feature appears at 527 eV, which is about 2 eV lower than the energy of the preedge peak in the pure $LaFeO_3$ system. This feature grows in intensity as the concentration of Ni increases. With the increase in intensity of this new feature, the relative intensity of the doublet structure decreases, and at 50% Ni substitution the doublet is hard to resolve from that of the $LaFeO_3$ and appears as a broad structure. The spectrum in the high energy region remains the same. To understand these observed features in our spectra from $x=0.1$ to $x=0.5$, we have compared our results with the results reported in literature on the pure $LaFeO_3$ and $LaNiO_3$ using Bremsstrahlung isochromat (BI) spectra, which can be easily compared with the x-ray absorption data.[8] As reported by Sarma *et al.*,[6] the spectral features for $LaFeO_3$, dominated by Fe $3d$ states, appear at 3 eV and 4.4 eV, whereas in the case of pure $LaNiO_3$ a narrow feature appear at 1 eV due to the existence of strong correlation effects within the metallic conduction band derived from the interaction between Ni $d$ and O $p$ states.[8] Similar effects have been observed in our O $K$-edge x-ray absorption spectra for Ni substituted samples. The clear distinction between the two peak, i.e., the peak from the Ni states and Fe states have been observed and the energy difference between them is also about 2 eV, as reported in BI spectra. It can also be seen from Fig. 4 that the Ni states' character dominates as the Ni substitution concentration is increased This indicates that the metallic conduction bandwidth is increasing, which is supported by our electrical transport studies showing a sharp decrease in resistance with the substitution of Ni in $LaFeO_3$. Accordingly, the activation energy also decreases. It is recalled here that Sarma *et al.*[16] have also investigated the XAS study of this series at O $K$ edge for the pure $LaFeO_3$ and for 30% and 50% of the Ni substitution in $LaFeO_3$ of our interest. Their findings are consistent with ours; however, we note that the spectra do not clearly resolve the spectral features of Fe and Ni ions distinctly, which may be due to the resolution ($\sim$0.4 eV). On the contrary, in the presented data the resolution is better than 0.2 eV, and hence we can clearly observe the evolution of the Ni $3d$ character as Ni concentration is increased in $LaFe_{1-x}Ni_xO_3$ as well as the distinct features of Fe $3d$ levels.

It is a well-known fact that the multiple valence states of $3d$ transition metals are characterized by x-ray absorption spectra measured at $L_{2,3}$ edges. The $3d$ transition metals also exhibit a valence-specific multiplet structures and chemical shift towards higher energy losses with increasing oxidation state.[24,25] Also, the $L_{2,3}$ edges are very strongly influenced by the core-hole potentials.[26,27] To understand the valence state of Fe and Ni in these samples and also the effect of core-hole potential, which changes with the Ni substitution in $LaFeO_3$, we have measured the x-ray absorption spectra of Fe $L_{2,3}$ edges. Figure 5 shows the Fe $L_{2,3}$ spectra of pure $LaFeO_3$ and Ni-substituted samples from $x=0.1$ to $x=0.5$, together with the spectra for $Fe_2O_3$ as reference. It is evident that the valence state of Fe in these compounds is +3 as their spectra have similar features with the $Fe_2O_3$ spectra. All these spectra show two broad multiplet structures, $L_3$ and $L_2$, separated by spin-orbit splitting of the Fe $2p$ core hole. The spectra can be very similar and, as Ni replaces Fe, the shoulderlike satellite structure becomes broader (inset in Fig. 5 shows the broadening of the $L_2$-edge XAS spectra features for the samples with $x=0.0$ and 0.5) which may be due to the increase in the delocalized nature of Fe $3d$ electrons. Also, the intensity is increasing with Ni concentration indicating the insulator-to-metallic behavior, which is consistent with the resistivity data. However, the valency of Fe remains consistently the same since the position of peak remains constant within the resolution of our measurements. Since there is interference of the La $M_{4,5}$ edge with the Ni $L_{2,3}$ edges, the data of Ni $2p$ is not presented and discussed. However, the La $M_{4,5}$-edge spectra (not shown here) resemble any other trivalent La.

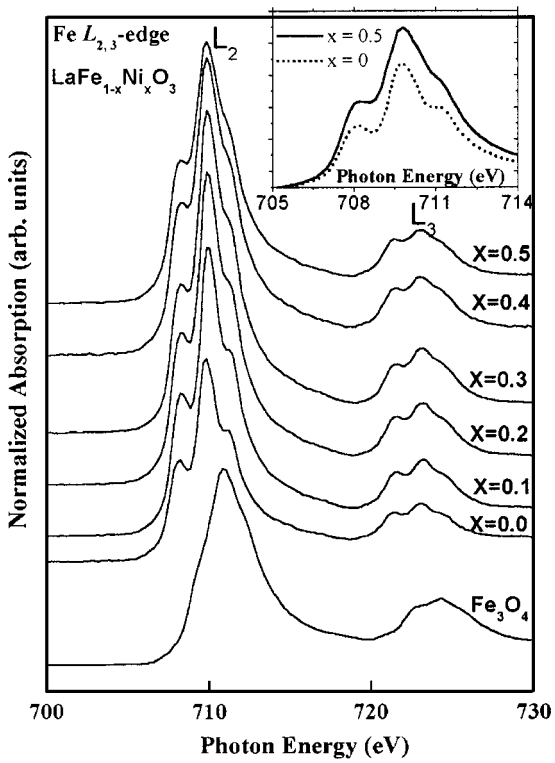


FIG. 5. Normalized Fe $L_{2,3}$-edge XAS spectra of $LaFe_{1-x}Ni_xO_3$ ($x=0.0$ to 0.5). The inset shows the $L_2$-edge XAS spectra features for the $x=0.0$ and 0.5 samples.

## IV. SUMMARY

To summarize, we have synthesized the single phase of $LaFe_{1-x}Ni_xO_3$ ($x\leqslant 0.6$) materials and studied their electronic structure using the x-ray appearance near-edge structure (XANES) spectra of O $K$, Fe $L_{2,3}$, and La $M_{4,5}$ edges. Upon substitution of Ni at Fe site in $LaFeO_3$, the O $K$-edge spectra show a new structure about 2.0 eV lower than that of $LaFeO_3$. This new feature is growing as the concentration of

Ni is increasing. This is consistent with the results of the resistivity data, which show that the resistivity decreases very fast from GΩ cm for $LaFeO_3$ to a few mΩ cm for the sample with 60% Ni substitution. The resistivity data have been analyzed using the variable-range hopping model and it is found that the gap parameter reduces systematically with the Ni substitution. This gap parameter decreases very systematically with the substitution concentration. The structural analysis also reveals that the samples exhibit single-phase orthorhombic structure with space group *Pnma* up to the 60% substitution level. From the Fe $L_{2,3}$-edge structures we have found that the Fe ions are in the trivalent state. The observed features have been explained on the basis of the charge-carrier doping in $LaFeO_3$. From the above-mentioned observations, it is evident that the disorder-induced localization is found to effectively control the resistivity behavior.

## ACKNOWLEDGMENTS

This work is supported by the Department of Science and Technology under Project No. SP/S2/M-07/98. The authors are thankful to Dr. Sudhindra Rayprol for helping in the XRD analysis. The authors (W.F.P. and K.A.) thank the National Science Council, Taiwan for financial support and NSRRC for technical support during XANES measurements. One of the authors (R.I.C.) would like to acknowledge CSIR for financial support.

[1]J. G. Bednorz and K. A. Muller, Z. Phys. B: Condens. Matter **64**, 189 (1986).
[2]R. von Helmont, J. Wecker, B. Holzaphel, L. Schultz, and K. Samwer, Phys. Rev. Lett. **71**, 2331 (1993).
[3]Y. Okimoto, T. Katsufuji, T. Ishikawa, A. Urushibara, T. Arima, and Y. Tokura, Phys. Rev. Lett. **75**, 109 (1995).
[4]D. D. Sarma, N. Shanthi, and P. Mahadevan, Phys. Rev. B **54**, 1622 (1996).
[5]I. Vobornik, L. Perfetti, M. Zacchigna, M. Grioni, G. Margaritondo, J. Mesot, M. Medarde, and P. Lacorre, Phys. Rev. B **60**, R8426 (1999).
[6]D. D. Sarma, N. Shanthi, S. R. Barman, N. Hamada, H. Sawada, and K. Terakura, Phys. Rev. Lett. **75**, 1126 (1995).
[7]Z. Y. Wu, M. Benfatto, M. Pedio, R. Cimino, S. Mobilio, S. R. Barman, K. Maiti, and D. D. Sarma, Phys. Rev. B **56**, 2228 (1997).
[8]J.-H. Park, T. Kimura, and Y. Tokura, Phys. Rev. B **58**, R13330 (1998).
[9]A. R. Moodenbaugh, B. Nielsen, S. Sambasivan, D. A. Fischer, T. Friessnegg, S. Aggarwal, R. Ramesh, and R. L. Peffter, Phys. Rev. B **61**, 5666 (2000).
[10]K. Asokan, K.V. R. Rao, J. C. Jan, J. W. Chiou, W. F. Pong, R. Kumar, S. Husain, and J. P. Srivastava, Surf. Rev. Lett. **9**, 1053 (2003).
[11]N. Y. Vasanthacharya, P. Ganguly, J. B. Goodenough, and C. N. R. Rao, J. Phys. C **17**, 2745 (1984).
[12]K. Sreedhar. J. M. Honig, M. Darwin, M. MvElfresh, O. M. Shand, J. Xu, B. C. Crooker, and J. Spalck, Phys. Rev. B **46**, 6382 (1992).
[13]P. Ganguly, N. Y. Vasanthacharya, C. N. R. Rao, and P. P. Edwards, J. Solid State Chem. **54**, 400 (1984).
[14]A. Chainani, D. D. Sarma, I. Das, and E. V. Sampathkumaran, J. Phys.: Condens. Matter **8**, L631 (1996).
[15]C. N. R. Rao, O. Prakash, and P. Ganguly, J. Solid State Chem. **15**, 186 (1975).
[16]D. D. Sarma, O. Rader, T. Kachel, A. Chainani, M. Mathew, K. Holldack, W. Gudat, and W. Eberhardt, Phys. Rev. B **49**, 14238 (1994).
[17]D. D. Sarma, A Chainani, S. R. Krishnakumar, E. Vescovo, C. Carbone, W. Eberhardt, O. Rader, Ch. Jung, Ch. Hellwig, W. Gudat, H. Srikanth, and A. K. Raychaudhuri, Phys. Rev. Lett. **80**, 4004 (1998).
[18]A. E. Bocquet *et al.*, Phys. Rev. B **45**, 1561 (1992).
[19]N. E. Massa, H. Falcon, H. Salva, and R. E. Carbonio, Phys. Rev. B **56**, 10178 (1997).
[20]A. E. Goeta, G. F. Goya, R. C. Mercader, G. Punte, H. Falcon, and R. Caronio, Hyperfine Interact. **90**, 371 (1994).
[21]K. Yoshi, H. Abe, N. M. Maskai, and A. Nakamura, *Proceedings of the Eighth International Conference on Ferrites (ICF8)* (Japan Society of Powder at Powder Metallurgy, 2000), p. 278.
[22]M. J. MacEachern, H. Dabkouska, J. D. Garrett, G. Amou, N. Gong, Guo Liu, and J. E. Greedan, Chem. Mater. **6**, 2092 (1994).
[23]A. Chainani, M. Mathew, and D. D. Sarma, Phys. Rev. B **48**, 14818 (1993).
[24]R. S. Liu, L. Y. Jang, J. M. Chen, J. B. Wu, R. G. Liu, J. G. Lin, and C. Y. Huang, Solid State Commun. **105**, 605 (1998).
[25]J. Kawai *et al.*, Spectrochim. Acta, Part B **55**, 1385 (2000).
[26]F. J. Mele and J. J. Ritsko, Phys. Rev. Lett. **43**, 68 (1979).
[27]J. Chaboy, M. Benfatto, and I. Davoli, Phys. Rev. B **52**, 10014 (1995).